

Engineering of extended focii for Optical Coherence Microscopy

Christophe Pache, Martin Villiger, Simon Rutishauser, Rainer A. Leitgeb and Theo Lasser

Laboratoire d'Optique Biomédicale, Ecole Polytechnique Fédérale de Lausanne, Lausanne, Switzerland

christophe.pache@epfl.ch

1. Introduction

So-called diffraction-free beams consist in solutions of the Helmholtz equation whose envelope of the electromagnetic field in the lateral directions is independent of the propagation distance [1].

Bessel beams belong to the family of these special field distributions. Theoretically such a beam carries an infinite amount of energy distributed evenly in its lobes over an infinite radial extent. However, in practice it is possible to generate finite-aperture approximations of Bessel beams exhibiting similar properties over a finite axial extent [2]. Due to their constant high intensity concentration over a relatively long propagation distance, these beams find their application in different areas, such as optical trapping [3], fluorescence microscopy [4] and Fourier Domain Optical Coherence Microscopy (FDOCM) [5].

There exist many methods to create zero order Bessel beams [6]. The axicon is certainly the most well-known and used technique. Circular diffraction gratings have also been developed to create such waves [7]. In this paper, we compare these two different methods to produce an extended depth of field for use in FDOCM based on simulations [8]. First we introduce the concept of the ideal extended focus.

2. Extended depth of field

To demonstrate the principle of an extended depth of focus, a simple setup focusing a collimated beam, as shown in Fig. 1, can be analyzed.

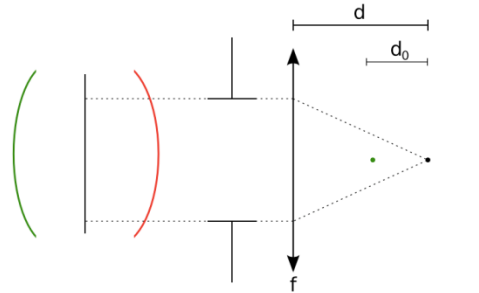
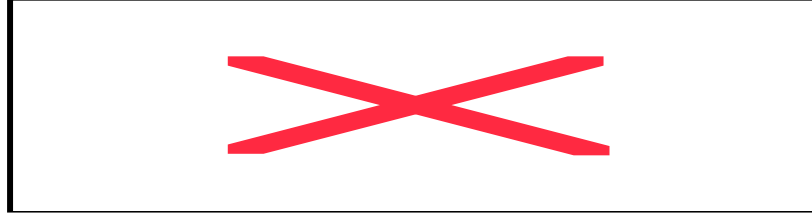


Fig. 1: Scheme of the multifocal setup: three beams having different defocus aberrations and their respective focal plane position in color. The green wavefront, which is converging will be focused before the focal of the lens. On the opposite, a divergent beam (in red) will produce a focal spot at a longer distance.

Consider a wavefront in the aperture plane consisting in the sum of several (infinitely) waves with different defocus aberrations, as produced by a lens of focal length F on a plane wave.

The phase φ of one component of the wavefront can be written as: $\varphi = \exp\left(-ik\rho^2/2F\right)$, where k is the wave vector and $\rho = \sqrt{x^2 + y^2}$ is the radial coordinate. The position of the focal plane d of this component is given by: $d = f - f^2/F$. When $|F| \gg f$, the effect of the defocusing lens is to move the focus position around the nominal focal length f by the distance $d_0 = f^2/F$.

To take into account a relative phase offset between the different components, the phase is fixed to be zero at $\rho = \rho_0$. The phase ϕ of the total wavefront corresponding to an extended focus from $f-d_0$ to $f+d_0$ is given by the integral of φ over d :



(1)

Eq. 1 shows that to produce an extended depth of focus, the phase of the incident wavefront on the focusing lens must follow an annular distribution in the aperture plane. The magenta line in fig. 2 on the left shows the annular pattern of this ideal extended focus. The middle plot shows the axial extent in the focal plane and on the right hand side the radial envelope.

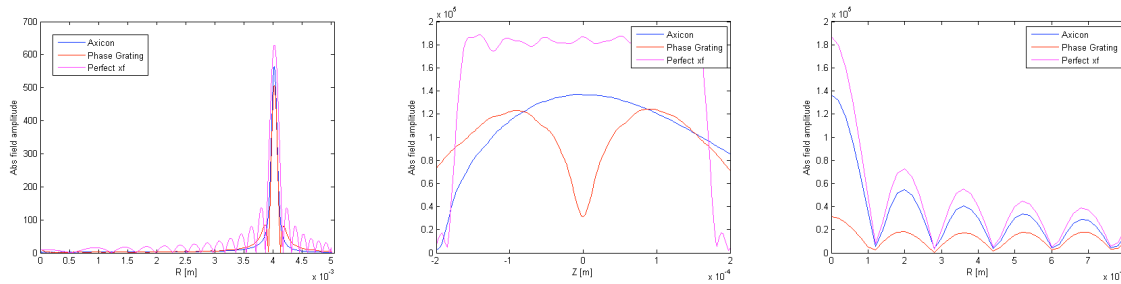


Fig. 2: Comparison of the ideal extended focus beam with practical realizations by the axicon and the annular phase grating.

3. Method

The simulation [6] computes the focal field distribution based on a Debye integral approach using the chirped z-transform for rapid computation. As an input, the field distribution in the input principle plane of the microscope objective is required. Fig. 3 shows the experimental layout of the different configurations. The plane wave propagation algorithm from the axicon and phase grating respectively to the principle plane of the objective we use a fast Hilbert transform. This first simulation step assumes radial symmetry and a scalar field. Only the second step takes polarization into account.

The transverse field distribution is calculated in two different locations, indicated in Fig. 2. In addition, the axial distribution of the focus field is also estimated, in order to compare the focal range of each method.

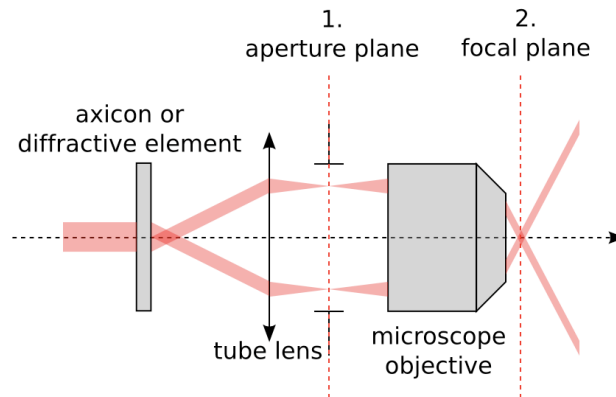


Fig. 3: Scheme of the Bessel illumination: planes 1 and 2 (aperture and focal planes) indicate the two locations where the transverse distribution of the field is compared

4. Preliminary results

Fig. 2 shows the field distributions in the mentioned locations. All fields show the expected annular pattern in the aperture plane. The ideal extended focus shows a nearly rectangular axial profile. The axial envelope of the axicon is

much smoother and has a long tail, spreading the energy along the axis and reducing the maximum amplitude. The pattern of the phase mask on the other hand shows an intensity minimum in the focal plane, with two lobes in the axial direction. Botcherby et al. [4] get rid of this minimum by apodizing the pattern in the aperture with an annular mask. However, FDOCM's broadband illumination creates a lateral spreading of the annular pattern in the aperture, as is shown in fig. 4 for some wavelengths, what makes this modification unsuitable for FDOCM.

The radial envelope in the focal plane on the other hand is very similar for all illumination schemes. Investigating its spectral dependence however, it is important to understand that the lateral spacing of the Bessel's zeros remains unaltered for the case of the phase mask. The wavelength dependent radius of the annulus in the aperture compensates the normal spectral focus variation. This dispersive effect is on the other hand pronounced in the case of the axicon illumination.

The signal reconstruction of FDOCM involves summation of the different spectral components. This is similar to a spectral averaging of the different observed radial profiles. In the case of the phase mask, this summation has no effect and results in the Bessel-like profile displayed in fig 4 on the right hand side. In case of the axicon, however, this summation results in a washout of the sidelobes, what is expected to have a positive impact on the tomogram.

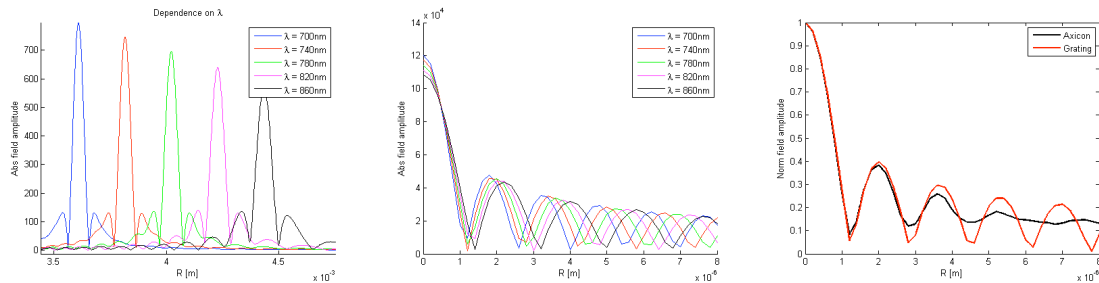


Fig.4: Focal field of a Bessel beam generated by an axicon

5. Conclusion

The use of Bessel beams for FDOCM increases the focal depth range with a constant transverse resolution [5]. This study presents a first comparison of some properties of Bessel beams, either generated by an axicon or a diffraction grating. There are still open questions to determine the most efficient method to create such beams for FDOCM.

6. References

- [1] Durnin et al., "Diffraction-free beams", Phys Rev Lett (1987) vol. 58 (15) pp. 1499-1501
- [2] Vasara et al. "Realization of general nondiffracting beams with computer-generated holograms", J Opt Soc Am A (1989) vol. 6 (11) pp. 1748-1754
- [3] McGloin et al. "Bessel beams: diffraction in a new light", Contemp Phys (2005) vol. 46 (1) pp. 15-28
- [4] Botcherby et al. "Scanning two photon fluorescence microscopy with extended depth of field", Opt Commun (2006) vol. 268 (2) pp. 253-260
- [5] Leitgeb et al. "Extended focus depth for Fourier domain optical coherence microscopy", Opt Lett (2006) vol. 31 (16) pp. 2450-2452
- [6] Herman et al. "Production and uses of diffractionless beams", J Opt Soc Am A (1991) vol. 8 (6) pp. 932-942
- [7] Reivelt et al. "Optical generation of focus wave modes", J Opt Soc Am A (2000) vol. 17 (10) pp. 1785-1790
- [8] Leutenegger et al. "Fast focus field calculations", Opt Express (2006) vol. 14 (23) pp. 11277-11291